

(Salen)Co(II)/*n*-Bu₄NX Catalysts for the Coupling of CO₂ and Oxetane: Selectivity for Cyclic Carbonate Formation in the Production of Poly-(trimethylene carbonate)

Donald J. Darensbourg* and Adriana I. Moncada

Department of Chemistry, Texas A&M University, College Station, Texas 77843

Received January 29, 2009; Revised Manuscript Received April 29, 2009

ABSTRACT: The (salen)Co(II) complex ((1*R*,2*R*)-(–)-1,2-cyclohexanediamino-*N,N'*-bis(3,5-di-*tert*-butyl-salicylidene)cobalt(II)) in the presence of an anion initiator, e.g. bromide, has been shown to be a very effective catalytic system for the coupling of oxetane and carbon dioxide, to provide the corresponding polycarbonate with minimal amount of ether linkages. The mechanism of the coupling of oxetane and carbon dioxide has been studied by in situ infrared spectroscopy, where the first formed product is trimethylene carbonate (TMC). TMC is formed by a backbiting mechanism following ring-opening of oxetane by the anion initiator, subsequent to CO₂ insertion into the cobalt–oxygen bond. The formation of the copolymer is shown to proceed mostly by way of the anionic ring-opening polymerization of preformed trimethylene carbonate in the presence of an anion in solution. Anions that are good leaving groups, i.e., bromide and iodide, are most effective at affording copolymer via this route. In the presence of greater than 2 equiv of anions the overall rate of copolymer production is decreased, presumably due to inhibition of oxetane monomer binding to the cobalt center. However, under these conditions copolymer formation through ROP of TMC is enhanced, with mass spectral evidence found for the formation of a dimer of TMC.

Introduction

Carbon dioxide is an abundant, inexpensive, easy to transport/store, and nontoxic biorenewable resource, which makes it an attractive C₁ feedstock to be used in several important industrial processes.¹ One growing area in CO₂ chemistry involves the production of polycarbonates via the alternating coupling of CO₂ and epoxides in the presence of metal-based catalysts,² a field pioneered by Inoue and co-workers in the late 1960s.³ This copolymerization process is often accompanied by the formation of varying amounts of ether linkages, which are the result of consecutive epoxide ring-opening. Additionally, five-membered cyclic carbonates are observable byproducts in these reactions, which are formed by a backbiting mechanism, thus shortening the polymer chain by one unit each occurrence. This latter event can be a major reaction pathway when utilizing aliphatic epoxides such as ethylene oxide, propylene oxide, and styrene oxide. Both polymeric and monomeric products obtained from the coupling of epoxides and carbon dioxide have important industrial applications. Polycarbonates have wide-scale uses in electronics, optical media, automotive, and medical industry. On the other hand, five-membered cyclic carbonates have numerous applications as high boiling and flash point solvents and also as reactive intermediates.⁴

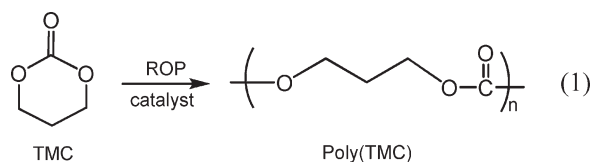
The formation of five-membered cyclic carbonates derived from the coupling reaction of epoxides and CO₂ has been extensively investigated using various types of catalysts. Homogeneous metal salen-based catalysts of aluminum,⁵ chromium,^{6,7} cobalt,⁸ zinc,^{8d} manganese,⁹ and tin¹⁰ have shown to have high catalytic activities. Similarly, aluminum complexes of phthalocyanines and porphyrins are also highly active catalysts.¹¹ Ionic liquids such as imidazolium salts have

also been reported as catalysts for the formation of cyclic carbonates from epoxides and carbon dioxide.¹² Moreover, the reaction of epoxides and CO₂ in molten quaternary ammonium bromide has been shown to afford cyclic carbonates.¹³ Furthermore, other metal complexes of nickel,¹⁴ ruthenium,¹⁵ zinc,¹⁶ and copper^{9b} have been similarly reported to be active catalysts for this transformation. Organic-based catalysts such as phenols¹⁷ and 4-(*N,N*-dialkylamino)pyridines¹⁸ have also been investigated. Recently, CO₂ adducts of *N*-heterocyclic carbenes were also demonstrated to be effective organic catalysts for these processes.¹⁹ In addition, heterogeneous-based materials such as Al–Mg mixed oxides,²⁰ magnesium oxide,²¹ and Cs-modified zeolites²² have been shown to be catalysts for this reaction, not only because of their high activity but also because these catalysts can be easily separated from the reaction solution and in most cases recycled.

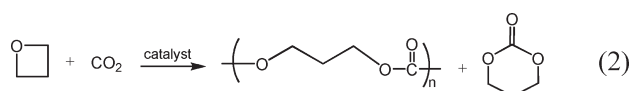
Five-membered cyclic carbonates are thermodynamically stable toward polycarbonate formation without loss of carbon dioxide. However, six-membered cyclic carbonates such as trimethylene carbonate (TMC or 1,3-dioxan-2-one) can under certain catalytic conditions undergo ring-opening polymerization to provide the corresponding polycarbonate, in this case poly(TMC), with complete retention of its CO₂ contents (eq 1). That is, the ring-opening polymerization of six- and seven-membered cyclic carbonates is spontaneous at all temperatures (ΔH_p is negative and ΔS_p is positive).⁴ Recently, there has been an intense interest for developing active catalytic systems for the process illustrated in eq 1.²³ The copolymer obtained by this method in general contains none or reduced ether linkages that may result from decarboxylation.^{24–26} These copolymers are biodegradable materials that have a wide range of potential biomedical applications, including sutures, drug delivery, and tissue

*Corresponding author: e-mail djdarens@mail.chem.tamu.edu; Fax (979) 845-0158.

engineering.²⁷ In addition, this strategy is industrially desirable because it can be performed as a melt process.



It is worth mentioning that trimethylene carbonate is readily obtained from 1,3-propanediol and ethyl chloroformate or diethyl carbonate.^{24,28} Therefore, it is of great interest to investigate greener routes for the production of this six-membered cyclic carbonate monomer. Conforming to this objective, the copolymerization of oxetane and carbon dioxide represents an attractive alternative (eq 2). In this instance, the six-membered cyclic carbonate byproduct, TMC, can be ring-opened and transformed into the same alternating copolymer by way of the reaction shown in eq 1.²⁹



Recently, our group has been investigating the mechanistic aspects of the copolymerization of oxetane and CO₂ catalyzed by (salen)CrCl complexes in the presence of *n*-Bu₄NX (X = Cl, N₃) as cocatalysts.^{30,31} Optimization of the catalytic system and catalytic conditions has led us to produce copolymers with 100% selectivity and ~97% carbonate linkages. Mechanistic and kinetic studies on this reaction showed that the formation of copolymer proceeded in part by way of the intermediacy of trimethylene carbonate and by the direct enchainment of oxetane and CO₂. As a consequence of our findings with the (salen)CrCl derivatives, we surmised that a decrease in the electrophilicity of the metal center in conjunction with the appropriate anionic initiator should tune the selectivity of the oxetane and CO₂ coupling process for cyclic carbonate formation and/or for copolymer produced directly from the homopolymerization of preformed TMC (Scheme 1). To examine this hypothesis, the commercially available catalyst (salen)Co(II)³² ((1*R*,2*R*)-(–)-1,2-cyclohexanediamino-*N,N'*-bis(3,5-di-*tert*-butylsalicylidene)cobalt(II)) (Figure 1) was employed in the presence of anionic-based cocatalysts derived from *n*-Bu₄NX (X = Cl, N₃, Br, I) salts. Included in this investigation is a mechanistic study of this process as monitored by in situ infrared spectroscopy. This correspondence encompasses an examination of cocatalyst dependence, substrate binding, and oxetane ring-opening.

Experimental Section

Reagents and Methods. Unless otherwise specified, all manipulations were carried out on a double-manifold Schlenk vacuum line under an atmosphere of argon or in an argon-filled glovebox.

(1*R*,2*R*)-(–)-1,2-Cyclohexanediamino-*N,N'*-bis(3,5-di-*tert*-butylsalicylidene)cobalt(II) was purchased from Strem Chemical. (Salen)CoBr was synthesized following the procedure published for the preparation of (salen)CoCl by Jacobsen and co-workers.³³ Toluene was freshly distilled from sodium/benzophenone. 1,1,2,2-Tetrachloroethane (TCE) was freshly distilled from CaH₂. Oxetane (Alfa Aesar) was freshly distilled from CaH₂ and stored in the freezer of the glovebox. Tetra-*n*-butylammonium bromide (Aldrich), tetra-*n*-butylammonium iodide (Eastman), and tetra-*n*-butylammonium chloride (TCI) were recrystallized from acetone/diethyl ether before used. Tetra-*n*-butylammonium azide (TCI) was stored in the freezer of the glovebox upon arrival. 4-(Dimethylamino)pyridine (DMAP, Aldrich) was recrystallized from ethanol/diethyl ether, and triethylamine (Fisher Scientific) was freshly distilled from CaH₂. Bone-dry carbon dioxide supplied in a high-pressure cylinder and equipped with a liquid dip tube was purchased from Scott Specialty Gases.

IR spectra were recorded on a Mattson 6021 Fourier transform (FT) IR spectrometer with a MCT detector. Molecular weight determinations (*M_n* and *M_w*) were carried out with a Viscotek Modular GPC apparatus equipped with ViscoGel I-series columns (H + L) and a model 270 dual detector comprised of refractive index and light scattering detectors. High-pressure reaction kinetic measurements were performed using an ASI ReactIR 1000 reaction analysis system with stainless steel Parr autoclave modified with a permanently mounted ATR crystal (SiComp) at the bottom of the reactor (purchased from Mettler Toledo).

Copolymerization Reactions of Oxetane and Carbon Dioxide.

Optimization of the Cocatalyst. In a typical experiment, 119 mg of complex **1**, the appropriate amount of cocatalyst, and 4 g of oxetane were delivered via the injection port into a 300 mL stainless steel Parr autoclave reactor that was previously dried in vacuo overnight at 80 °C. The autoclave was then pressurized with 35 bar of CO₂, and the temperature was increased to 110 °C. The monomer:catalyst:cocatalyst ratio was maintained at 350:1:2, and the reaction was run for 24 h. After the reaction was stopped, the autoclave was put into ice and cooled down to 10 °C. A ¹H NMR spectrum of the reaction mixture was taken to determine the percent conversion to polymer, and after removal of the unreacted monomer, to determine the percentages of poly (TMC), ether linkages, and TMC at 4.23, 3.50, and 4.43 ppm in CDCl₃, respectively.

Copolymerization Reactions Monitored by in Situ IR Spectroscopy. In a typical experiment, complex **1** (277 mg), the appropriate amount of *n*-Bu₄NBr, and oxetane (4 g) were dissolved in 10 mL of toluene and delivered via the injection port into a 300 mL stainless steel Parr autoclave reactor that was previously dried in vacuo overnight at 80 °C and cooled down to room temperature. The autoclave is modified with a 30 bounce SiComp window to allow for the use of an ASI ReactIR 1000 system equipped with a MCT detector. In this manner a 128-scan background spectrum was collected after the reaction mixture was heated to the temperature of the corresponding experiment. The autoclave was pressurized with 35 bar of CO₂, and the infrared spectrometer was set to collect one spectrum every 3 min over a 24 h period. Profiles of the absorbance

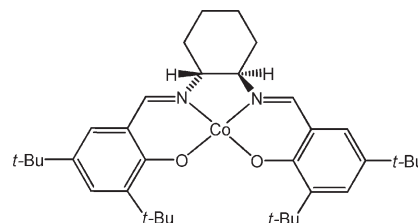
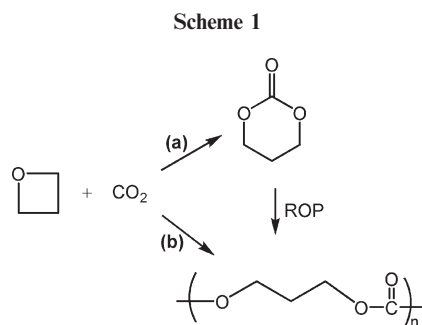


Figure 1. The (salen)Co(II) complex **1** employed in the present studies, (1*R*,2*R*)-(–)-1,2-cyclohexanediamino-*N,N'*-bis(3,5-di-*tert*-butylsalicylidene)cobalt(II).

at 1750 cm^{-1} (polymer) and at 1770 cm^{-1} (TMC) with time were recorded after baseline correction.

Cocatalyst, Substrate Binding, and Ring-Opening Step Examined by Infrared Spectroscopy. Cocatalyst, substrate binding, and ring-opening step studies were examined by solution infrared spectroscopy. The catalytic system used in these studies was complex **1** in the presence of $n\text{-Bu}_4\text{NN}_3$ as cocatalyst and using TCE as the solvent.

Statistical Deconvoluted of FTIR Spectra. Where noted FTIR spectra were deconvoluted using Peakfit, version 4.12 (Peakfit for Windows, v. 4.12; SYSTAT Software Inc., San Jose, CA, 2003). Statistical treatment was a residuals method utilizing a combination Gaussian–Lorentzian summation of amplitudes with a linear baseline and Savitsky–Golay smoothing.

Ring-Opening Polymerization of Trimethylene Carbonate

Control Experiments. In a typical experiment, the appropriate amounts of TMC, complex **1**, and/or $n\text{-Bu}_4\text{NBr}$ were weighted out in a Schlenk flask in a monomer:catalyst:cocatalyst ratio of 300:1:2 followed by the addition of 30 mL of toluene. The reaction vessel was placed into a preheated oil bath at 110 $^\circ\text{C}$ and stirred. The percent conversion to polymer was obtained by analyzing the sample solution by ^1H NMR spectroscopy.

Results and Discussion

Our initial study was to employ the (salen)Co(II) catalyst, complex **1**, in the presence of various cocatalysts to investigate the catalytic activity and selectivity for cyclic carbonate vs copolymer formation from the coupling of oxetane and carbon dioxide. The chiral version of complex **1** was employed in this study because of its commercial availability. Since there is not an opportunity for asymmetry in the copolymer produced, a racemic catalyst would suffice. The copolymerization reactions were performed under identical reaction conditions, i.e., 110 $^\circ\text{C}$ and 35 bar of CO_2 pressure. The results are summarized in Table 1. The product mixtures were analyzed by ^1H NMR spectroscopy, with the quantities of poly(TMC), TMC, and ether linkages in poly(TMC) determined by integrating the resonances at 4.23, 4.43, and 3.50 ppm, respectively. As is readily seen in Table 1, both products poly(TMC) and TMC were obtained with the use of bromide- and iodide-based cocatalysts, and the yield of poly(TMC) was much greater than that of the cyclic product (entries 1 and 2, Table 1). Among the ionic-based cocatalysts examined, the bromide anion displayed the highest catalytic activity (entry 1, Table 1). The iodide, chloride, and azide anions were found to be significantly less effective (entries 2–4, Table 1). The catalytic activity of this system largely depended on the counteranion of the cocatalyst used, and the order of decreasing activity was $\text{Br}^- > \text{I}^- > \text{Cl}^- > \text{N}_3^-$. A similar trend has been observed by Endo for the coupling of carbon dioxide or carbon disulfide and aziridines employing alkali metal halides or tetraalkylammonium halides as catalysts.³⁴ In addition, Caló reported the coupling of oxiranes and CO_2 to produce cyclic carbonates in the presence of molten tetra-*n*-butylammonium bromide as catalyst.¹³

It was also of interest to investigate the catalytic activity of amine-based cocatalysts such as DMAP and triethylamine for this process. It has been reported in the literature that these types of initiators in the presence of cobalt-, zinc-, copper-, chromium-, and tin-based catalysts are active for the formation of cyclic carbonates from the coupling of propylene oxides and CO_2 .^{7,8c,10,35} In contrast, triethylamine and DMAP were found to be ineffective for the coupling of oxetane and CO_2 in the presence of complex **1** (entries 5 and 6, Table 1), most likely due to the difficulty of these amine-based cocatalysts to ring-open oxetane.

We have shown that oxetane ring-opening is a higher energy process than the corresponding reaction involving epoxides,^{30,31} and thus a good nucleophile would be required for this step. On the other hand, the formation of TMC, which is most likely caused by a backbiting mechanism, needs a good leaving group (Scheme 2). It is worth mentioning at this point that in the case of the tetraalkylammonium halide-based cocatalysts studied the tetraalkylammonium cation is weakly interacting, and hence the anions are freer for ring-opening the monomer. The order of decreasing nucleophilicity of the anions, in a polar aprotic media (neat oxetane) and in a nonpolar solvent (such as toluene, as it will be shown later), is $\text{N}_3^- \sim \text{Cl}^- > \text{Br}^- > \text{I}^-$. The bromide anion, being in the middle of the series, is promoting the formation of the cyclic product better than the iodide, chloride, and azide ions. The iodide anion is the best leaving group among the series, but at the same time it is a poorer nucleophile and does not as readily facilitate the ring-opening reaction. On the contrary, the azide and chloride anions are the better nucleophiles but are the poorer leaving groups of the series, and as a result they do not drive the reaction to the formation of the cyclic carbonate product. Of importance to point out at this time is that the formation of copolymer is evident with the use of the bromide anion, and its mechanism of formation will be discussed *vide infra*.

Scheme 2

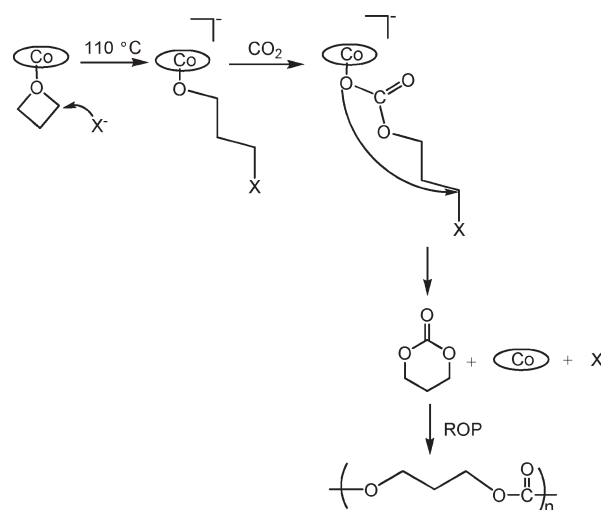


Table 1. Copolymerization of Oxetane and CO_2 Catalyzed by Complex **1** in the Presence Various Cocatalysts^a

entry	cocatalyst	% conversion ^b	% poly(TMC) ^b	% TMC ^b	% CO_2 content ^b
1	$n\text{-Bu}_4\text{NBr}^c$	68.4	93.3	6.7	98.4
2	$n\text{-Bu}_4\text{NI}$	13.9	93.0	7.0	97.6
3	$n\text{-Bu}_4\text{NCl}$	6.4	100	0	> 99
4	$n\text{-Bu}_4\text{NN}_3$	1.4	100	0	> 99
5	DMAP	0.44	0	100	> 99
6	triethylamine	1.06	0	100	> 99

^a Copolymerization conditions: 119 mg of catalyst, 4 g of oxetane, $\text{M/I} = 350:1$, 2 equiv of cocatalyst, 35 bar of CO_2 , at 110 $^\circ\text{C}$ for 24 h. ^b Percent conversion to products, product distributions, and % of CO_2 content were determined by ^1H NMR spectroscopy. ^c $M_n(\text{GPC}) = 7560$, $\text{PDI} = 1.56$, $M_n(\text{theoretical}) = 22\,852$.

Cocatalyst, Substrate Binding, and Ring-Opening Step Examined by Solution Infrared Spectroscopy. Fundamental to a better understanding of the mechanism of the coupling reaction of oxetane and carbon dioxide catalyzed by (salen)Co(II)/*n*-Bu₄NBr is an investigation of the initiation step of this process. For this purpose, cocatalyst/substrate binding and ring-opening step studies carried out using solution infrared spectroscopy in TCE were designed to address this issue. For the solution infrared spectroscopy studies we utilized (salen)Co(II), complex **1**, along with the azide anion derived from the very soluble *n*-Bu₄NN₃, since the ν_{N_3} stretching vibration provides accessible probes for both anion metal binding and ring-opening steps.

The infrared spectrum of complex **1** in the presence of 2 equiv of *n*-Bu₄NN₃ revealed that most of the azide anion remained uncoordinated to the metal center. That is, a large absorbance of free N₃[−] at 2009 cm^{−1} was observed with only a weak absorbance at 2052 cm^{−1} assignable to (salen)CoN₃[−] being seen. Similarly, upon addition of 3 equiv of *n*-Bu₄NN₃, there was an increase in the extent of azide binding to cobalt(II) as indicated by an increase in the absorbance at 2052 cm^{−1} with a concomitant decrease in the ν_{N_3} mode at 2009 cm^{−1} due to free azide. Subsequent addition of an 100-fold excess of oxetane to the solution resulted in an increase intensity of the metal bound azide vibrational mode at ~2052 cm^{−1}, presumably due to (salen)CoN₃·oxetane[−]. Upon heating the solution at 110 °C an organic azide vibration was noted at 2100 cm^{−1} which grew in intensity as the free and metal bound azide frequencies decreased in intensity. These observations are best summarized in Scheme 3.

On the other hand, upon changing the cyclic ether to tetrahydrofuran, at an 100-fold excess to (salen)Co, the extent of formation of (salen)CoN₃·THF[−] was seen to be significantly lower than in the oxetane analogous process. This is consistent with the lower basicity of tetrahydrofuran compared to that of oxetane ($\text{p}K_{\text{b}}$ of tetrahydrofuran = 5.00, $\text{p}K_{\text{b}}$ of oxetane = 3.13).³⁶ That is, in the presence of a less basic ether ligand, the formation of a stable octahedral (salen)Co(II)(N₃)(THF)[−] adduct is diminished.

Cocatalyst Dependence on the Copolymerization of Oxetane and CO₂ Catalyzed by (salen)Co(II)/*n*-Bu₄NBr. After examining the initiation step of the copolymerization process, we have undertaken an investigation into the cocatalyst (anion) concentration dependence of the copolymerization process in order to further optimize the catalytic system. These reactions were performed in toluene solution in the presence of complex **1** along with varying amounts of *n*-Bu₄NBr. The reactions were monitored by in situ infrared spectroscopy by observing the growth of the copolymer's $\nu_{\text{C=O}}$ band at 1750 cm^{−1} as well as the growth and/or consumption of the TMC's $\nu_{\text{C=O}}$ band at 1770 cm^{−1}. The three-dimensional plots for poly(TMC) formation, and TMC formation and consumption, along with their corresponding reaction profiles are shown in Figures 2–4. It can be seen that the rate for the production of poly(TMC) is the highest when 2 equiv of *n*-Bu₄NBr are utilized (Figure 2). The product distribution for the copolymerization reactions performed using varying amounts of *n*-Bu₄NBr are shown in Table 2. Consistent with the in situ IR data, the best

catalytic activity is obtained when 2 equiv of *n*-Bu₄NBr are employed (entry 2, Table 2). The use of 1 equiv of cocatalyst was found to be detrimental to the overall process (entry 1, Table 2), where just a 8.2% conversion was obtained.

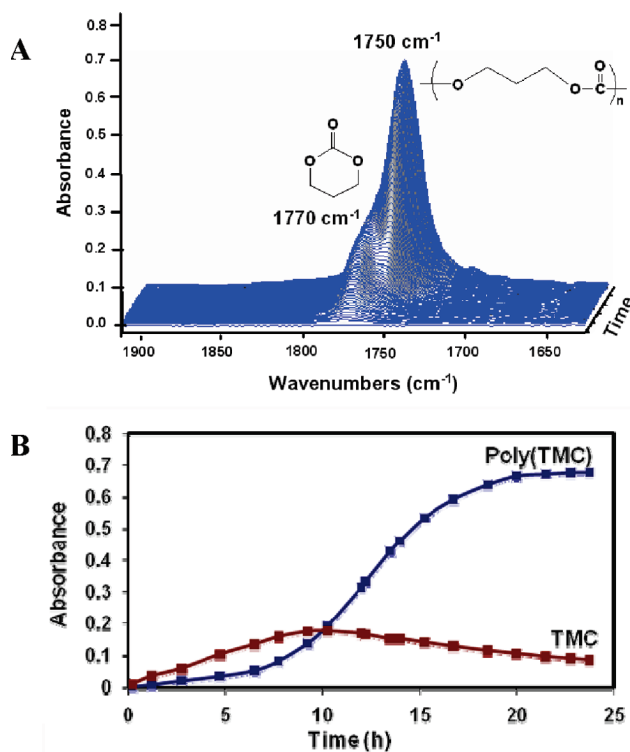


Figure 2. (A) Three-dimensional stack plot of the IR spectra collected every 3 min during the copolymerization reaction of oxetane and CO₂. Reaction carried out at 110 °C in toluene at 35 bar CO₂ pressure, using complex **1** along with 2 equiv of *n*-Bu₄NBr. (B) Reaction profile for poly(TMC) and TMC, obtained after deconvolution of selected IR spectra.

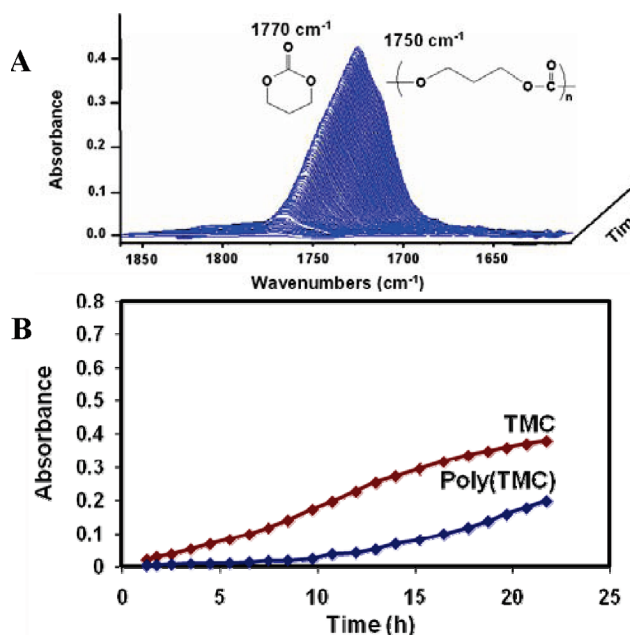
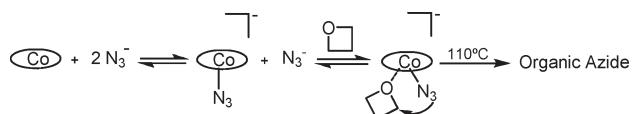


Figure 3. (A) Three-dimensional stack plot of the IR spectra collected every 3 min during the copolymerization reaction of oxetane and CO₂. Reaction carried out at 110 °C in toluene at 35 bar CO₂ pressure, using complex **1** along with 3 equiv of *n*-Bu₄NBr. (B) Reaction profile for poly(TMC) and TMC, obtained after deconvolution of selected IR spectra.

Scheme 3



The use of more than 2 equiv of cocatalyst enhanced the production of TMC over that of poly(TMC), but the catalytic activity is decreased (entries 3 and 4, Table 2). The decrease in rate of oxetane conversion upon increasing the bromide ion concentration is likely due to competitive binding of bromide vs the oxetane monomer to the cobalt center. At this time it is not clear why 5 equiv of bromide ion result in higher conversion as compared to 3 equiv. Further studies, including attempts to kinetically model these consecutive reactions, will be explored. Unfortunately, this process is complicated by difficulties in measuring the disappearance of oxetane at high pressures and hydrolysis of bromide end groups in the polymer resulting from ROP of TMC by adventitious water. The reactions depicted in Figures 3 and 4 with 3 and 5 equiv of *n*-Bu₄NBr, respectively, were carried out for an additional 24 h, resulting in an increase in the ratio of poly(TMC) to TMC as would be anticipated.

The reaction solution obtained from the experiment performed employing (salen)Co(II) with 5 equiv of *n*-Bu₄NBr was further analyzed by electron-spray ionization mass spectroscopy. The parent ions of (TMC + Li)⁺ and (2TMC + Li)⁺ (Figure 5) were observed in the positive mode of the ESI-mass spectrum at 109.04 and 211.07 *m/z*,

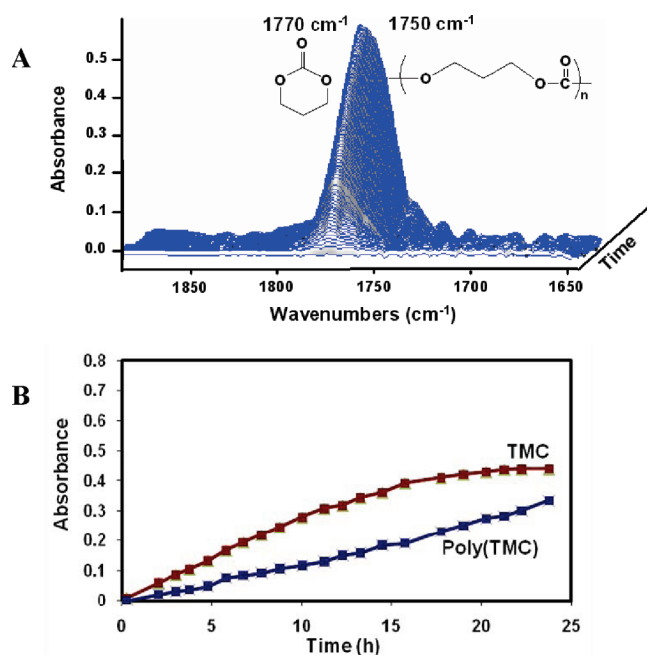


Figure 4. (A) Three-dimensional stack plot of the IR spectra collected every 3 min during the copolymerization reaction of oxetane and CO₂. Reaction carried out at 110 °C in toluene at 35 bar CO₂ pressure, using complex 1 along with 5 equiv of *n*-Bu₄NBr. (B) Reaction profile for poly(TMC) and TMC, obtained after deconvolution of selected IR spectra.

Table 2. Copolymerization of Oxetane and CO₂ Catalyzed by Complex 1 in the Presence of Varying Quantities of *n*-Bu₄NBr^a

equiv of cocatalyst	% conversion ^b	% poly (TMC) ^b	% TMC ^b	% CO ₂ content ^b
1	8.2	53.5	46.5	> 99
2 ^c	64.0	95.2	4.8	97.3
3	28.8	32.2	67.8	> 99
5	46.7	20.9	79.1	> 99

^a Copolymerization conditions: 277 mg of catalyst, 4 g of oxetane, 10 mL of toluene, M/I = 150:1, 35 bar of CO₂, at 110 °C for 24 h. ^b Percent conversion to products, product distributions, and % of CO₂ content were determined by ¹H NMR spectroscopy. ^c *M_n*(GPC) = 4215, PDI = 1.64, *M_n*(theoretical) = 9344.

respectively. This result strongly suggests that larger size cyclic backbiting products are possible during the reaction. Pertinent to this point, single crystals of trimethylene carbonate were isolated from the reaction solution and characterized by X-ray crystallography (Figure 6). The structure of trimethylene carbonate has been reported by Kataeva and co-workers in the gas phase by electron diffraction and in solution using the Kerr effect and dipole moments.³⁷ The metric parameters for TMC are similar to those previously reported but are of greater accuracy with *R*₁ = 0.0277, *R*_w = 0.0753, and a goodness-of-fit of 1.017. Crystallographic data pertaining to this crystal structure are provided in Table 3, with selected bond distances and angles provided in Table 4.

Polymer Characterization. Relevant to our mechanistic studies for copolymer formation was the characterization of the polymers by ¹H NMR spectroscopy and their molecular weight determinations by gel permeation chromatography. In general, the observed *M_n* values of the copolymers obtained from the coupling of oxetane and CO₂ in the presence of (salen)Co(II)/*n*-Bu₄NBr were found to be much lower than the expected theoretical values. This is most likely due to a chain transfer mechanism arising from the presence of trace quantities of water in the system.³⁸

It was of interest to carefully analyze the copolymers obtained from oxetane/CO₂ by ¹H NMR spectroscopy to determine whether the copolymers contained ether linkages. We have previously shown that copolymers obtained from the ring-opening polymerization of TMC catalyzed by (salen)CrCl complexes in the presence of *n*-Bu₄NN₃ contained no ether linkages. On the other hand, by utilizing the same catalyst system, copolymers obtained from oxetane/CO₂ showed minimal amounts of ether linkages.³⁰ Figure 7 illustrates the ¹H NMR spectrum of a purified polycarbonate sample obtained from the copolymerization of oxetane and carbon dioxide. Purification of the copolymer was achieved by precipitation from a dichloromethane solution with 1 M HCl in methanol, followed by vacuum drying. In general, a small amount of ether linkages are observed in the copolymers (~1.1%), which strongly suggests, that oxetane is ring-opened during polymer chain growth.

The presence of ether linkages was further confirmed by treatment of the polymer with trifluoroacetic anhydride in CDCl₃ (Figure 7). Trifluoroacetic anhydride reacts rapidly

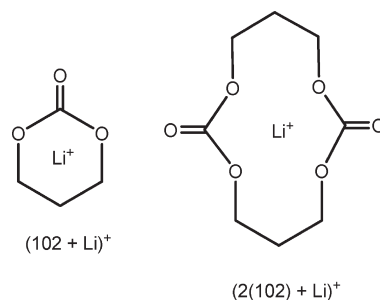


Figure 5. Lithium adducts of TMC and dimeric TMC.

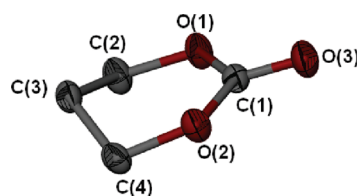


Figure 6. Thermal ellipsoid plot of trimethylene carbonate. Ellipsoids are at the 50% level. H atoms are omitted for clarity.

Table 3. Crystallographic Data for Trimethylene Carbonate

empirical formula	C ₄ H ₆ O ₃
fw	102.09
temperature (K)	110(2) K
crystal system	monoclinic
space group	<i>P</i> 2 ₁ / <i>n</i>
<i>a</i> (Å)	6.097(6)
<i>b</i> (Å)	11.306(11)
<i>c</i> (Å)	6.734(7)
α (deg)	90.0
β (deg)	102.259(11)
γ (deg)	90.0
<i>V</i> (Å ³)	453.6(8)
<i>D_c</i> (mg/m ³)	1.495
<i>Z</i>	4
abs coeff (mm ⁻¹)	0.130
reflections collected	3668
independent reflections	708 [<i>R</i> (int) = 0.0277]
restraints/parameters	0/64
GOF on <i>F</i> ²	1.017
final <i>R</i> indices [<i>I</i> > 2 σ (<i>I</i>)]	^a <i>R</i> ₁ = 0.0277 ^b <i>R</i> _w = 0.0753
final <i>R</i> indices (all data)	^a <i>R</i> ₁ = 0.0286 ^b <i>R</i> _w = 0.0762

Table 4. Selected Bond Distances and Angles for Trimethylene Carbonate^a

O(1)–C(1)	1.3296(18)
O(1)–C(2)	1.4545(17)
O(3)–C(1)	1.2056(15)
C(2)–C(3)	1.4910(19)
C(1)–O(2)–C(4)	120.97(10)
O(3)–C(1)–O(2)	119.73(12)
O(1)–C(1)–O(2)	120.44(9)
O(1)–C(2)–C(3)	110.91(11)
C(2)–C(3)–C(4)	107.47(10)

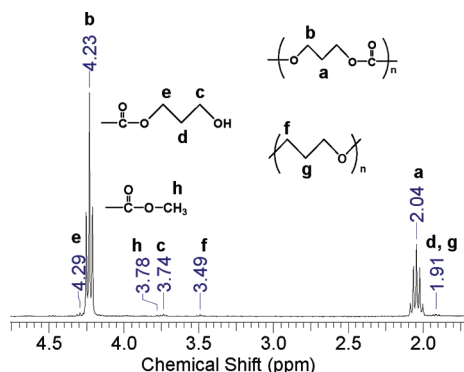
^a Units of bond angles and bond distances are deg and Å, respectively.

Figure 7. ¹H NMR spectrum in CDCl₃ of poly(TMC) obtained by way of oxetane/CO₂, in the presence of (salen)Co(II)/*n*-Bu₄NBr as the catalytic system. Polymer was purified from dichloromethane and 1 M HCl solution in methanol.

with –OH end groups of the polymers, with the signal of the resulting –CH₂O–C(O)CF₃ end groups showing up around 0.5 ppm downfield relative to the –CH₂OH end groups. In a similar manner, a downfield shift of about 0.1–0.15 ppm of the ether linkages is expected, and indeed, it was observed after the addition of the trifluoroacetic anhydride. Kricheldorf has reported this method as a way to identify –CH₂OH end groups and ether linkages in poly(TMC) samples. The downfield shift of the ether linkages was attributed to hydrogen bonding between the oxygen of ether linkages and the liberated trifluoroacetic acid byproduct. In good accordance with this interpretation was the increase of the downfield shift of the ether linkages with higher concentrations of trifluoroacetic acid observed by Kricheldorf.²⁶ Ether linkages which are observed at 3.50 ppm may be overlapping with –CH₂Br end

Table 5. Control Experiments to Examine Copolymer Formation^a

entry	monomer	% conversion ^b	<i>M_n</i> (GPC)	<i>M_n</i> (theoretical)	PDI
1	oxetane/CO ₂				
2	TMC ^c	78.11	29 512	23 902	1.68
3	TMC ^c	87.23	28 917	26 692	1.68
4	TMC ^d	89.78	25 025	27 473	1.63
5	TMC ^d	88.14	22 053	26 971	1.66

^a Reaction conditions: oxetane/CO₂ run: 4 g of oxetane, M/I = 350:1, 2 equiv of *n*-Bu₄NBr, 35 bar of CO₂, at 110 °C for 24 h. TMC runs (entries 2 and 4): 0.5 g TMC, M/I = 300:1, 2 equiv of *n*-Bu₄NBr, 30 mL of toluene, at 110 °C. TMC runs (entries 3 and 5): 0.5 g TMC, M/I = 300:1, 10 mg of complex **1**, 2 equiv of *n*-Bu₄NBr, 30 mL of toluene, at 110 °C. ^b Percent conversion to polymer was determined by ¹H NMR spectroscopy. ^c Reaction time = 1 h. ^d Reaction time = 4 h.

groups in the copolymer, which are expected to show at 3.5 ppm as well. However, –CH₂Br end groups were not detectable by ¹H NMR.

Mechanistic Insight into the Oxetane and Carbon Dioxide Coupling Process. At this point it is beneficial to summarize our findings on the copolymerization reaction. First, trimethylene carbonate production via a backbiting mechanism is evident as definitively shown by in situ infrared spectroscopy. Furthermore, although ring-opening polymerization of *preformed* trimethylene carbonate accounts for much of the copolymer production under certain conditions, at least some copolymer formation results from direct oxetane incorporation into the growing polymer chain. Prior to putting forth a complete mechanistic scheme for copolymer formation, it remains for us to assess the conditions for trimethylene carbonate ring-opening to copolymer. A series of control experiments were designed to address this issue, and these are found in Table 5.

Initially, a copolymerization run was performed under identical conditions as described before but in the absence of the (salen)Co(II) complex, i.e., 4 g of oxetane, 35 bar of CO₂, 110 °C, and *n*-Bu₄NBr as the catalyst. Under these conditions no copolymer was produced after a 24 h period (entry 1, Table 5). In addition, two control experiments were performed for the ring-opening polymerization of TMC, utilizing 0.5 g of TMC, 2 equiv of *n*-Bu₄NBr, in the presence and absence of complex **1**, reaction temperature 110 °C (Table 5, entries 2 and 3). As readily seen in Table 5, the percent conversion to polymer obtained from the reaction where complex **1**/*n*-Bu₄NBr was employed as the catalyst system was slightly higher than that where *n*-Bu₄NBr was employed alone (entries 2 and 3). Similarly, longer reaction times (4 h) produced closer percent conversion to polymer (entries 4 and 5). Importantly, after only 4 h of reaction TMC is converted to polymer in high percent conversions in both instances. On the other hand, the coupling of oxetane and CO₂ catalyzed by (salen)Co(II)/*n*-Bu₄NBr requires a much longer reaction time (24 h) under similar reaction conditions to obtain around 64% conversion to polymer. This reaction time difference further supports the role of (salen)Co(II) on the coupling reaction. Therefore, (salen)Co(II) complex catalyzes the formation of TMC by a backbiting mechanism, and the resultant TMC undergoes ring-opening polymerization by an anionic mechanism with the bromide anions in solution.

Scheme 4 summarizes the proposed mechanistic aspects for the coupling reaction of oxetane and carbon dioxide catalyzed by (salen)Co(II)/*n*-Bu₄NBr catalyst, based on our current experimental findings. In the initiation step, treatment of (salen)Co(II) with 2 equiv of *n*-Bu₄NBr, and in the presence of oxetane monomer, a (salen)Co(II)Br·(oxetane)[–] adduct is formed. Following the initial ring-opening of oxetane by bromide and CO₂ insertion into the resultant

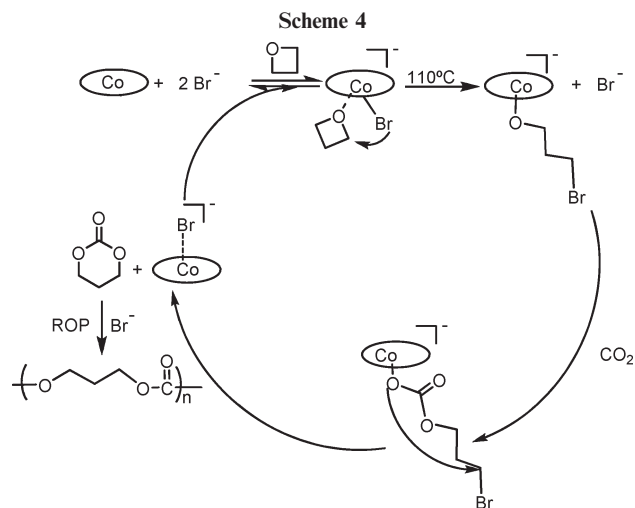


Table 6. Selectivity for Poly(TMC) and TMC Formation Using (Salen)CoBr Complex in the Presence of *n*-Bu₄NBr as the Cocatalyst^a

Salen cobalt(III) complex	cocatalyst	% conversion ^b	% poly (TMC) ^b	% TMC ^b	% CO ₂ content ^b
(salen)CoBr	<i>n</i> -Bu ₄ NBr (1 equiv)	34.37	32.93	67.02	> 99
(salen)CoBr ^c	<i>n</i> -Bu ₄ NBr (2 equiv)	62.28	41.52	58.47	> 99

^a Copolymerization conditions: 157 mg of catalyst, 2 g of oxetane, M/I = 150:1, 35 bar of CO₂, at 110 °C for 24 h. ^b Percent conversion to products, product distributions and % of CO₂ content were determined by ¹H NMR spectroscopy. ^c *M*_n(GPC) = 6284, PDI = 1.68, *M*_n(theoretical) = 3960.

cobalt–oxygen bond, the formation of TMC by a backbiting process with ring closure is evident. Regeneration of a (salen)CoBr[−] species is then followed by oxetane binding to the cobalt center, and the catalytic cycle starts over. Moreover, ring-opening polymerization of preformed TMC may be carried out by an anionic mechanism in the presence of bromide anion in solution to yield poly(TMC). Furthermore, it is important to note that oxetane insertion into the polymer chain occurs, which generates small amounts of ether linkages in the copolymer.

Since (salen)CoX complexes in the presence of quaternary organic salts have been shown to be effective catalyst systems under mild reaction conditions, it was of interest to examine this catalyst for the copolymerization of oxetane and CO₂.^{26,39,40} For this study the (salen)CoCl complex along with anionic initiators from *n*-Bu₄NX or PPNX (X = Cl or N₃) was utilized. The polymerization reactions were performed under identical reaction conditions to those employed in the (salen)Co(II) investigation, i.e., 110 °C and 35 bar CO₂ pressure. Under these conditions no copolymer was obtained after 24 h, and upon lowering the reaction temperature to 50 °C no improvement in catalytic activity was noted. However, upon changing to (salen)CoBr in the presence of *n*-Bu₄NBr catalytic activity was observed, with the results indicated in Table 6.

As noted in Table 6, the percent conversion to products, poly(TMC) and TMC, increases upon increasing the number of equivalents of *n*-Bu₄NBr from 1 to 2 equiv. This observation, coupled with the lack of catalytic activity seen for the chloride and azide catalyst analogues, is consistent with what is observed when utilizing (salen)Co(II) complexes as catalysts. Indeed, upon quenching the copolymerization process, a red solid precipitates which was identified as (salen)Co(II).

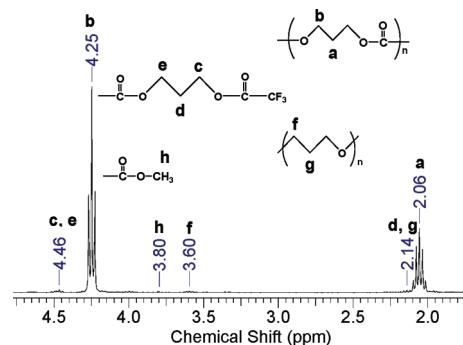


Figure 8. ¹H NMR spectrum in CDCl₃ of poly(TMC) obtained by way of oxetane/CO₂, in the presence of (salen)Co(II)/*n*-Bu₄NBr as the catalytic system. Polymer was purified from dichloromethane and 1 M HCl solution in methanol and treated with trifluoroacetic anhydride.

Recall, (salen)CoX complexes are a deep green in color. This behavior of (salen)CoX complexes operating at elevated temperatures has been previously observed numerous times.^{2c} Hence, copolymerization reactions of oxetane and CO₂ at 110 °C employing (salen)CoX/*n*-Bu₄NX catalyst systems proceed via the mechanism described in Scheme 4 for the (salen)Co(II) complex.

Concluding Remarks

We initially chose the (salen)Co(II) catalyst for the coupling of oxetanes and carbon dioxide because of its reduced electrophilicity and substitutional lability relative to (salen)CrX complexes. That is, (salen)Co(II) should have less of a tendency to bind the growing polymer chain, thus leading to an enhanced rate of cyclization of the free anionic CO₂ inserted ring-opened monomer or oligomer. As has been documented, the metal center in (salen)CoX is also less electrophilic than that in (salen)CrX; however, noted herein and elsewhere, (salen)CoX complexes are unstable with regard to reduction to (salen)Co under the required reaction conditions of elevated temperatures. An unanswered issue in this study is whether the metal's only involvement is to activate the oxetane for ring-opening. In other words, does CO₂ insertion occur at the metal center, or does CO₂ simply react with the dissociated alkoxide resulting from ring-opened oxetane?

Acknowledgment. We gratefully acknowledge the financial support from the National Science Foundation (CHE 05-43133) and the Robert A. Welch Foundation (A-0923).

Supporting Information Available: X-ray crystallographic files in CIF format for the structure determination of trimethylene carbonate (TMC). This material is available free of charge via the Internet at <http://pubs.acs.org>.

References and Notes

- (1) Aresta, M.; Dibenedetto, A. *Catal. Today* **2004**, *98*, 455–462.
- (2) (a) Chisholm, M. H.; Zhou, Z. *J. Mater. Chem.* **2004**, *14*, 3081–3092. (b) Cohen, C. T.; Chu, T.; Coates, G. W. *J. Am. Chem. Soc.* **2005**, *127*, 10869–10878. (c) Darensbourg, D. J. *Chem. Rev.* **2007**, *107*, 2388–2410. (d) Darensbourg, D. J.; Holtcamp, M. W. *Coord. Chem. Rev.* **1996**, *153*, 155–174. (e) Darensbourg, D. J.; Mackiewicz, R. M.; Phelps, A. L.; Billodeaux, D. R. *Acc. Chem. Res.* **2004**, *37*, 836–844. (f) Kuran, W. *Prog. Polym. Sci.* **1998**, *23*, 919–992. (g) Moore, D. R.; Coates, G. W. *Angew. Chem., Int. Ed.* **2004**, *43*, 6618–6639. (h) Paddock, R. L.; Nguyen, S. T. *Macromolecules* **2005**, *38*, 6251–6253. (i) Sugimoto, H.; Inoue, S. *J. Polym. Sci., Part A: Polym. Chem.* **2004**, *42*, 5561–5573. (h) Super, M. S.; Beckman, E. J. *Trends Polym. Sci.* **1997**, *5*, 236–240.
- (3) Inoue, S.; Koinuma, H.; Tsuruta, T. *J. Polym. Sci., Part B: Polym. Phys.* **1969**, *7*, 287–292.

- (4) Clements, J. H. *Ind. Eng. Chem. Res.* **2003**, *42*, 663–674.
- (5) (a) Lu, X. B.; Feng, X. J.; He, R. *Appl. Catal. A* **2002**, *234*, 25–33. (b) Lu, X. B.; He, R.; Bai, C. X. *J. Mol. Catal. A: Chem.* **2002**, *186*, 1–11. (c) Lu, X. B.; Zhang, Y. J.; Jin, K.; Luo, L. M.; Wang, H. *J. Catal.* **2004**, *227*, 537–541. (d) Lu, X. B.; Zhang, Y. J.; Liang, B.; Li, X.; Wang, H. *J. Mol. Catal. A: Chem.* **2004**, *210*, 31–34.
- (6) Darensbourg, D. J.; Fang, C. C.; Rodgers, J. L. *Organometallics* **2004**, *23*, 924–927.
- (7) Paddock, R. L.; Nguyen, S. T. *J. Am. Chem. Soc.* **2001**, *123*, 11498–11499.
- (8) (a) Chen, S. W.; Kawthekar, R. B.; Kim, G. J. *Tetrahedron Lett.* **2007**, *48*, 297–300. (b) Lu, X. B.; Liang, B.; Zhang, Y. J.; Tian, J. Z.; Wang, Y. M.; Bai, C. X.; Wang, H.; Zhang, R. *J. Am. Chem. Soc.* **2004**, *126*, 3732–3733. (c) Shen, Y. M.; Duan, W. L.; Shi, M. *J. Org. Chem.* **2003**, *68*, 1559–1562. (d) Tanaka, H.; Kitaichi, Y.; Sato, M.; Ikeno, T.; Yamada, T. *Chem. Lett.* **2004**, *33*, 676–677.
- (9) (a) Jutz, F.; Grunwaldt, J. D.; Baiker, A. *J. Mol. Catal. A: Chem.* **2008**, *279*, 94–103. (b) Srivastava, R.; Bennur, T. H.; Srinivas, D. *J. Mol. Catal. A: Chem.* **2005**, *226*, 199–205.
- (10) Jing, H.; Edulji, S. K.; Gibbs, J. M.; Stern, C. L.; Zhou, H.; Nguyen, S. T. *Inorg. Chem.* **2004**, *43*, 4315–4327.
- (11) (a) Kasuga, K.; Kabata, N.; Kato, T.; Sugimori, T.; Handa, M. *Inorg. Chim. Acta* **1998**, *278*, 223–225. (b) Kasuga, K.; Nagao, S.; Fukumoto, T.; Handa, M. *Polyhedron* **1996**, *15*, 69–72. (c) Sugimoto, H.; Inoue, S. *Pure Appl. Chem.* **1998**, *70*, 2365–2369.
- (12) (a) Kawanami, H.; Sasaki, A.; Matsui, K.; Ikushima, Y. *Chem. Commun.* **2003**, 896–897. (b) Peng, J.; Deng, Y. *New J. Chem.* **2001**, *25*, 639–641.
- (13) Caló, V.; Nacci, A.; Monopoli, A.; Fanizzi, A. *Org. Lett.* **2002**, *4*, 2561–2563.
- (14) Li, F.; Xia, C.; Xu, L.; Sun, W.; Chen, G. *Chem. Commun.* **2003**, 2042–2043.
- (15) Man, M. L.; Lam, K. C.; Sit, W. N.; Ng, S. M.; Zhou, Z.; Lin, Z.; Lau, C. P. *Chem. Eur. J.* **2006**, *12*, 1004–1015.
- (16) Kim, H. S.; Bae, J. Y.; Lee, J. S.; Kwon, O.-S.; Jelliarko, P.; Lee, S. D.; Lee, S. H. *J. Catal.* **2005**, *232*, 80–84.
- (17) Shen, Y. M.; Duan, W. L.; Shi, M. *Adv. Synth. Catal.* **2003**, *345*, 337–340.
- (18) Shiels, R. A.; Jones, C. W. *J. Mol. Catal. A: Chem.* **2007**, *160*–166.
- (19) Zhou, H.; Zhang, W. Z.; Liu, C. H.; Qu, J. P.; Lu, X. B. *J. Org. Chem.* **2008**, *73*, 8039–8044.
- (20) Yamaguchi, K.; Ebitani, K.; Yoshida, T.; Yoshida, H.; Kaneda, K. *J. Am. Chem. Soc.* **1999**, *121*, 4526–4527.
- (21) Yano, T.; Matsui, H.; Koike, T.; Ishiguro, H.; Fujihara, H.; Masakuni, Y.; Maeshima, T. *Chem. Commun.* **1997**, 1129–1130.
- (22) Tu, M.; Davis, R. J. *J. Catal.* **2001**, *199*, 85–91.
- (23) (a) Darensbourg, D. J.; Choi, W.; Ganguly, P.; Richers, C. P. *Macromolecules* **2006**, *39*, 4374–4379. (b) Darensbourg, D. J.; Choi, W.; Karroonnirun, O.; Bhuvanesh, N. *Macromolecules* **2008**, *41*, 3493–3502. (c) Darensbourg, D. J.; Choi, W.; Richers, C. P. *Macromolecules* **2007**, *40*, 3521–3523. (d) Darensbourg, D. J.; Ganguly, P.; Billodeaux, D. R. *Macromolecules* **2005**, *38*, 5406–5410. (e) Mindermak, J.; Hilborn, J.; Bowden, T. *Macromolecules* **2007**, *40*, 3515–3517. (f) Nederberg, F.; Lohmeijer, B. G. G.; Leibfarth, F.; Pratt, R. C.; Choi, J.; Dove, A. P.; Waymouth, R. M.; Hedrick, J. L. *Biomacromolecules* **2007**, *8*, 153–160. (g) Yang, J.; Yu, Y.; Li, Q.; Li, Y.; Cao, A. *J. Polym. Sci., Part A: Polym. Chem.* **2005**, *43*, 373–384.
- (24) Ariga, T.; Takata, T.; Endo, T. *Macromolecules* **1997**, *30*, 737–744.
- (25) Kricheldorf, H. R.; Weegen-Schulz, B. *Macromolecules* **1993**, *26*, 5991–5998.
- (26) Kricheldorf, H. R.; Weegen-Schulz, B. *Polymer* **1995**, *36*, 4997–5003.
- (27) (a) Albertsson, A. C.; Eklund, M. *J. Polym. Sci., Part A: Polym. Chem.* **1994**, *32*, 265–279. (b) Pêgo, A. P.; Siebum, B.; VanLuyn, M. J. A.; Gelleo, K. J.; Van Seijen, Y.; Poot, A. A.; Grijpma, D. W.; Feijen, J. *Tissue Eng.* **2003**, *9*, 981–994.
- (28) Carothers, W. H.; Natta, F. J. V. *J. Am. Chem. Soc.* **1930**, *52*, 314–326.
- (29) (a) Baba, A.; Kashiwagi, H.; Matsuda, H. *Tetrahedron Lett.* **1985**, *26*, 1323–1324. (b) Baba, A.; Kashiwagi, H.; Matsuda, H. *Organometallics* **1987**, *6*, 137–140. (c) Baba, A.; Meishou, H.; Matsuda, H. *Makromol. Chem., Rapid Commun.* **1984**, *5*, 665–668. (d) Pritchard, J. G.; Long, F. A. *J. Am. Chem. Soc.* **1958**, *80*, 4162–4165.
- (30) Darensbourg, D.; Moncada, A. I.; Choi, W.; Reiebenspies, J. H. *J. Am. Chem. Soc.* **2008**, *130*, 6523–6533.
- (31) Darensbourg, D. J.; Moncada, A. I. *Inorg. Chem.* **2008**, *47*, 10000–10008.
- (32) Leung, W. H.; Chan, E. Y. Y.; Chow, E. K. F.; Williams, I. D.; Peng, S. M. *J. Chem. Soc., Dalton Trans.* **1996**, 1229–1236.
- (33) Nielsen, L. P. C.; Stevenson, C. P.; Blackmond, D. G.; Jacobsen, E. N. *J. Am. Chem. Soc.* **2004**, *126*, 1360–1362.
- (34) Sudo, A.; Morioka, Y.; Koizumi, E.; Sanda, F.; Endo, T. *Tetrahedron Lett.* **2003**, *44*, 7889–7891.
- (35) (a) Paddock, R. L.; Hiyama, Y.; McKay, J. M.; Nguyen, S. T. *Tetrahedron Lett.* **2004**, *45*, 2023–2026. (b) Paddock, R. L.; Nguyen, S. T. *Chem. Commun.* **2004**, 1622–1623.
- (36) Yamashita, Y.; Tsuda, T.; Okada, M.; Iwatsuki, S. *J. Polym. Sci., Part A: Polym. Chem.* **1966**, *4*, 2121–2135.
- (37) Kataeva, O. N.; Litvinov, I. A.; Naumov, V. A. *Zh. Strukt. Khim.* **1988**, *29*, 186–188.
- (38) (a) Darensbourg, D. J.; Fitch, S. B. *Inorg. Chem.* **2007**, *46*, 5474–5476. (b) Nakano, K.; Kamada, T.; Nozaki, K. *Angew. Chem., Int. Ed.* **2006**, *45*, 7274–7277.
- (39) Lu, X. B.; Shi, L.; Wang, Y. M.; Zhang, R.; Zhang, Y. J.; Peng, X. J.; Zhang, Z. C.; Li, B. *J. Am. Chem. Soc.* **2006**, *128*, 1664–1674.
- (40) Coates, G. W.; Cohen, C. T. *J. Polym. Sci., Part A: Polym. Chem.* **2006**, *44*, 5182–5191.